The Discrete Orthogonal Stockwell Transforms For Infinite-Length Signals And Their Real-Time Implementations

Yusong Yan
School of Information and Electronics
Beijing Institute of Technology
Beijing, China
yanys@bit.edu.cn

Hongmei Zhu
Department of Mathematics and Statistics
York University
Toronto, ON, Canada
hmzhu@yorku.ca

***Abstract*—In recent literature, the discrete Stockwell Transform (DST) for infinite length signals has been introduced along with its fast implementation. This method allows for low computational cost and enables processing of an infinite-length or large-size signal segment-by-segment while overcoming the boundary effects produced by conventional DST. The algorithm also preserves the absolute-reference phase, making it suitable for real-time signal processing. In this paper, we propose a new formulation of the discrete Orthogonal Stockwell Transform for infinite length signals. Based on the definition, we implement its fast algorithm using FFT. Our proposed scheme can process an infinite signal segment-by-segment, eliminating boundary effects and preserving the absolute-reference phase. Compared to the DST for infinite length signals, the DOST version significantly reduces computational complexity, making it more practical for real-time signal processing.**

Keywords—Infinite-length signals, the discrete Stockwell transforms, the discrete Orthogonal Stockwell transforms, real-time signal processing

I. INTRODUCTION

The Stockwell Transform (ST [1]) is a time-frequency technique that was developed in 1996. It allows for the simultaneous representation of a temporal signal using both time and frequency variables. By combining the short-time Fourier transform and wavelet transforms, the ST provides a multi-scale time-frequency representation of a signal while also maintaining the absolute-reference phase information consistent with the Fourier phase of the signal. This feature, along with its easy-to-interpret time-frequency spectrum and its close connection to the Fourier transform, has made the ST a widely-used tool in geophysics, biomedicine, oceanology, and the energy industry [2-8].

However, due to the high redundancy in its time-frequency representation, computing the full ST is highly intensive. Variations of the discrete STs (DSTs), such as the discrete orthogonal ST (DOSTs, [9-11]) and the generalized discrete ST (GDST)[12-14], were developed to reduce the computational complexity as well as to preserve the absolute-reference phase property.

All the discrete STs found in literature are designed to process finite-length signals. However, in applications such as audio, medical, and radar signal processing, the signal length may be large or even infinite. As the signal length increases, so does the number of frequency samples required for computation. This can exceed computational memory and storage capacity, making it difficult to compute the ST for such signals in a reasonable amount of time. While it is possible to compute the ST segment-by-segment, doing so results in boundary effects that wrap around the two ends of each segment and can distort the interpretation of local signal behavior. To address this issue, we proposed new DST transforms for infinite-length signals in [23]. These transforms eliminate boundary effects and preserve absolute-referenced phase. Furthermore, they can be implemented efficiently with low computational complexity and reasonable time delay, meeting the real-time system design requirements. However, the information redundancy in the DST for the infinite-length signals is still high, causing intensive computation.

Hence, in this paper, we present an extension of the discrete orthogonal Stockwell Transform (DOST) transform for infinite-length signals, with the aim of reducing information redundancy in the time-frequency representation and further increasing computational efficiency. The paper is organized as follows: In Section 2, we first derive the formula for the continuous ST of an infinitely sampled signal [23]. Then, we sample the time-frequency domain to formulate the DOST transform for an infinite-length signal. We also demonstrate that applying these formulae to periodic extensions of finite-length signals yields the conventional formulation of the DOST for finite-length signals [9-11]. Efficient numerical implementation of the infinite DOST is developed in Section 3. In Section 4, we provide numerical validation of our algorithm and analyze its computational complexities. Finally, we present further discussions and conclusions in Section 5.

II. THE CONTINUOUS STOCKWELL TRANSFORM AND ITS DISCRETIZATIONS

Mathematically, the continuous ST [1] for a continuous signal g(t) is defined as:

$$S(\tau,\upsilon)=\int_{-\infty}^{+\infty} g(t)w(\tau-t,\sigma)e^{-2\pi i t\upsilon}dt \quad (1)$$

Here, t is the time variable, and υ is the frequency variable. The window function $w(t,\sigma)$ is localized at time τ, where $\sigma=\sigma(\nu)$ is frequency-dependent and controls the window width. When the window function is Gaussian and $\sigma=\frac{1}{|\nu|}$, Equation (1) produces the conventional ST. We will show that discretizing the continuous ST spectrum will lead to the definition of the DST for both finite and infinite-length signals.

A. Sampling for ST Transform

First, we sample the continuous signal g(t) with an impulse sampling function with a sampling interval T and obtain the infinitely sampled signal $g'(t)$

$$g'(t) = \sum_{n=-\infty}^{+\infty} g(t)\,\delta(t-nT). \quad (2)$$

Substituting $g'(t)$ into Equation (1) gives the continuous ST spectrum of the sampled signal：

$$S'(\tau,\upsilon) = \int_{-\infty}^{+\infty} g'(t) w(\tau-t,\sigma) e^{-2\pi i t\upsilon} dt$$
$$= \sum_{n=-\infty}^{+\infty} g(nT)\cdot w(\tau-nT,\sigma)e^{-2\pi i nT\upsilon} \quad (3)$$

Here, both τ and υ are continuous variables. The function $S'(\tau,\upsilon)$ is periodic along the frequency variable υ with a period of $\frac{1}{T}$. However, it is not necessarily periodic along the time variable τ.

B. The DOST for Infinite-length Signals

Similar to obtaining DST[23] through sampling, this paper employs another way to sample the continuous S-spectrum $S'(\tau,\upsilon)$ and obtain the DOST. Let $N = 2^K$. For every integer $k \in [0,K]$, we select the following frequency sampling points:

$$\upsilon_k = \begin{cases} k/(NT) & k = 0,1, \\ 1/(2T) & k = K \\ (2^{k-1}+2^{k-2})/(NT) & k = 2...K-1 \end{cases}$$

For every given frequency sampling point υ_k, the time sampling points are chosen as:

$$\tau_l = \begin{cases} lNT & k = 0,1,K \\ l\frac{N}{2^{k-1}}T & k = 2..K-1 \end{cases} \quad \text{for } l \in [-\infty,\infty],$$

Then sampling the continuous S-spectrum $S'(\tau,\upsilon)$ at the sampling points (τ_l,υ_k) gives

$$S[l,k] = S'(\tau_l,\upsilon_k)$$
$$= \begin{cases} \sum_{n=-\infty}^{+\infty} g(nT)\cdot w(l\cdot NT-nT,\sigma)e^{-\frac{2\pi ink}{N}} & k=0,1 \\ \sum_{n=-\infty}^{+\infty} g(nT)\cdot w(l\cdot NT-nT,\sigma)e^{-\frac{2\pi in}{2}} & k=K \\ \sum_{n=-\infty}^{+\infty} g(nT)\cdot w(l\cdot 2^{K-k+1}T-nT,\sigma)e^{-\frac{2\pi in(2^{k-1}+2^{k-2})}{N}} & k=2...K-1 \end{cases}$$
$$= \begin{cases} \sum_{n=-\infty}^{+\infty} g[n]\cdot e^{-\frac{2\pi ink}{N}}\cdot w[l\cdot N-n,k] & k=0,1 \\ \sum_{n=-\infty}^{+\infty} g[n]\cdot e^{-\frac{2\pi in}{2}}\cdot w[l\cdot N-n,k] & k=K \\ \sum_{n=-\infty}^{+\infty} g[n]\cdot e^{-\frac{2\pi in(2^{k-1}+2^{k-2})}{N}}\cdot w[l\cdot 2^{K-k+1}-n,k] & k=2...K-1 \end{cases}$$

(6)

To simplify Equation (6), we define the frequency band width β as:

$$\beta = \begin{cases} 1 & k = 0,1,K \\ 2^{k-1} & k = 2...K-1 \end{cases},$$

the center frequency (i.e, the center of each frequency band) as

$$\upsilon = \begin{cases} k & k = 0,1 \\ N/2 & k = K \\ \frac{3}{2}\beta & k = 2...K-1 \end{cases}$$

and the time indices for time sampling points as：

$$\tau = \begin{cases} l\cdot N & k = 0,1,K \\ l\cdot 2^{K-k+1} & k = 2...K-1 \end{cases} \quad l \in [-\infty,\infty].$$

We can then rewrite Equation (6) as

$$S[l,k] = S[\upsilon,\beta,\tau] = \sum_{n=-\infty}^{+\infty} g[n]\cdot e^{-\frac{2\pi in\upsilon}{N}}\cdot w[\tau-n,\upsilon] \quad (7)$$

Using Equation (7), we define the DOST for an infinity-length discrete time signal g[n].

C. The DOST for Finite-length Signals

Similar to the conventional DST, for a given finite-length signal g[n] with support $[0, N-1]$， we periodically extend the signal to the entire domain. Then the convolution operator is equivalent to a circular convolution:

$$S[l,k] = \sum_{n=0}^{N-1} g[n]\cdot e^{-\frac{2\pi in\upsilon}{N}}\cdot w[\tau-n,k] \quad (8)$$

Using FFT, we can design a fast algorithm to compute Equation (8):

$$S[l,k] = FFT^{-1}\left(FFT\left(\sum_{n=0}^{N-1} g[n]\cdot e^{-\frac{2\pi in\upsilon}{N}}\cdot w[\tau-n,k]\right)\right)$$

If the window function satisfies $FFT(w[n,k]) = \Pi_{[-\frac{\beta}{2},\,\frac{\beta}{2}-1]}(m)$, where $\Pi_\Omega(m)$ is the rectangular function defined as the following

$$\Pi_\Omega(m) = \begin{cases} 1 & m \in \Omega + pN \\ 0 & m \notin \Omega + pN \end{cases}$$

Then we obtain

$$S[l,k] = FFT^{-1}\left(G[m+\upsilon]\cdot \Pi_{[-\frac{\beta}{2},\,\frac{\beta}{2}-1]}(m)\right)\Big|_\tau$$
$$= \sum_{m=0}^{N-1} G[m+\upsilon]\cdot \Pi_{[-\frac{\beta}{2},\,\frac{\beta}{2}-1]}(m) e^{2\pi i\frac{m\tau}{N}}$$
$$= \begin{cases} G[k] & k = 0,1 \\ G[N/2] & k = K \\ \sum_{m=-\beta/2}^{\beta/2-1} G[m+\upsilon]\cdot e^{2\pi i\frac{m\cdot l}{2^{k-1}}} & k = 2...K-1 \end{cases}$$
$$= \begin{cases} G[k] & k = 0,1 \\ G[N/2] & k = K \\ IFFT_\beta(G[m+\frac{3}{2}\beta]) & k = 2...K-1 \end{cases} \quad (8')$$

Equation (8') is exactly the conventional DOST that has been used in the literature for finite-length signals.

To summarize, we have formulated the DOST for both finite and infinite-length signals. While their algebraic formulations are similar, with one involving a sum from 0 to N-1 and the other involving an infinite sum from $-\infty$ to ∞, both methods generate a discrete time-frequency spectrum of a discrete time signal. Nonetheless, they differ significantly in theory.

The conventional DOST [10-12] uses circular convolution, which implicitly treats any finite-length signal as a periodic signal. This results in the beginning of the signal is wrapped around the end, creating discontinuities at the intersections of the ends and producing boundary effects that distort the spectrum. On the other hand, the new DOST formulation involves a sum from $-\infty$ to ∞ and is designed specifically to process infinite-length signals. Unlike the conventional DOST, the infinite-length DOST does not involve periodic extension and naturally eliminates boundary effects.

When using the FFT to compute the conventional DOST spectrum, the average computational complexity increases with the signal size N and can quickly exceed the capabilities of an average computer. However, the definition of the DOST of infinite-length signals given by Equation (7) reveals that the total number of frequency sampling points K is independent of the signal size. Therefore, the computational complexity of each signal point remains constant throughout the entire signal processing. This characteristic is essential for a real-time system.

In the next section, we will present low-cost computational methods for accurately computing the DOST time-frequency spectrum of an infinite-length signal.

III. The Discrete Orthogonal Stockwell Transform And Its Fast Implementation For Infinite-Length Signals

Equations (6) and (7) reformulate the DOST for infinite-length signals:

$$S[l,k] = S[\upsilon,\beta,\tau] = \sum_{n=-\infty}^{+\infty} g[n]\cdot e^{-\frac{2\pi i n \upsilon}{N}}\cdot w[\tau-n,\upsilon]$$

Like the DST, the DOST can be viewed as a process of frequency modulation $e^{-\frac{2\pi i n \upsilon}{N}}$ followed by an FIR filter w[n,m].

Thus, computing the DOST in Equation (6) is equivalent to filter a frequency modulated signal using a FIR filter of order N, similar to the DST proposed in [23]. This filtering can be realized efficiently in the frequency domain by partitioning the signal into overlapped segments of length 2N and then apply the Fourier transform on these segments.

Unlike the DST, the DOST does not employ uniform time sampling for different center frequency υ. Therefore, different FFT lengths must be used for different center frequencies.

Theorem 1: Given an N-length segment of an infinity signal, computation of the DOST for the segment with fixed frequency υ, bandwidth β and time sampling interval N/β, can be simplified as computing 2β-point FFT and the sum of 2N multiplications.

Proof:

$$S[l,k] = S[\upsilon,\beta,\tau] = \sum_{n=0}^{2N-1} g[n]\cdot e^{-\frac{2\pi i n \upsilon}{N}}\cdot w[\tau-n,\upsilon]$$

$$= FFT^{-1}\left(FFT\left(\sum_{n=0}^{2N-1} g[n]\cdot e^{-2\pi i\frac{n\upsilon}{N}}\cdot w[\tau-n,\upsilon]\right)\right)$$

$$= FFT^{-1}\left(FFT\left(\left(g[n]\cdot e^{-2\pi i\frac{n\upsilon}{N}}\right)\circledast w[n,\upsilon]\right)\right)$$

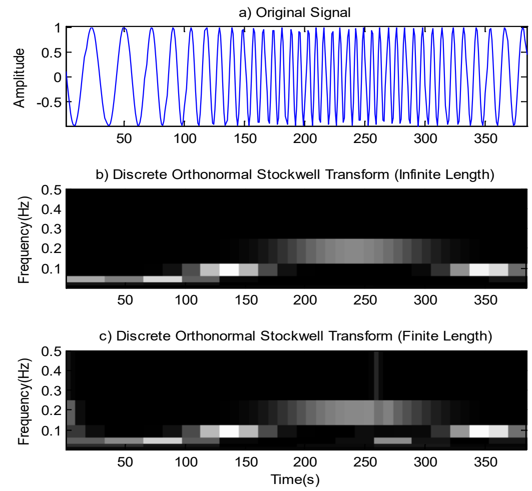

Fig. 1. *The time-frequency representation given by the discrete orthogonal Stockwell-transform for an infinite-length signal: a) 384 sample points of a non-stationary time signal whose frequency vary over time periodically; here, the sampling rate is 1Hz; b) the magnitude of the time-frequency spectrum of the portion of the signal as displayed in a) calculated by the infinite-length DOST; c) the magnitude of the time-frequency spectrum calculated by the finite-length DOST.*

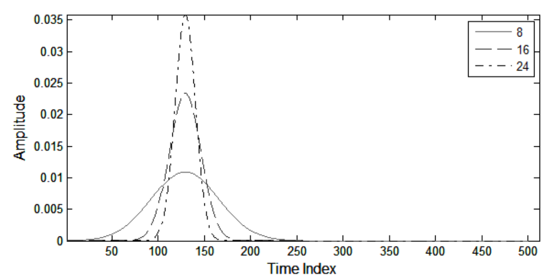

Fig. 2. *The window functions used in the DST for frequency indices 8, 16, and 24. The support of the function is 256 and the center of the window is $\tau = 128$. Note that we pad 256 zeros to the filter coefficients to form a filter B of length 512.*

$$= FFT^{-1}\left(FFT\left(g[n]\cdot e^{-2\pi i\frac{n\upsilon}{N}}\right)\cdot FFT(w[n,\upsilon])\right)$$

$$= FFT^{-1}(G[m+2\upsilon]\cdot W[m,\upsilon])$$

$$= \sum_{m=0}^{2N-1} G[m+2\upsilon]\cdot W[m,\upsilon]\cdot e^{2\pi i\frac{m\tau}{2N}}$$

Since $\tau = l\cdot\frac{N}{\beta}$, $l \in [0, 1, 2, \ldots 2\beta-1]$, then we have

$$S[l,k] = S[\upsilon,\beta,\tau] = \sum_{m=0}^{2N-1} G[m+2\upsilon]\cdot W[m,\upsilon]\cdot e^{2\pi i\frac{ml}{2\beta}}$$

$$= \sum_{m=0}^{2\beta-1}\left(\sum_{n=0}^{N/\beta-1} G[m+2n\beta+2\upsilon]\cdot W[m+2n\beta,\upsilon]\right)\cdot e^{2\pi i\frac{ml}{2\beta}}$$

■

Theorem 1 can be used to compute the DOST for infinite-length signals. For each signal segment of length N and each frequency, the DOST uses 2N multiplication and 2β-point FFT to compute, given the time sampling period is N/β.

Based on Theorem 1, we can derive the fast algorithm to compute the DOST of an infinite-length signal segment-by-segment:

Algorithm 1. Real-time Implementation for the DOST of An Infinite-length Signal

1) For a fixed center frequency υ, partition the frequency modulated signal b[n] into small segments. The k-th segment is

$$b_k[n] = b[kN+n] = g[kN+n] \cdot e^{-2\pi i\frac{(kN+n)\upsilon}{N}},$$

For simplicity, we denote

$$b_k[n] = g_k[n] e^{-2\pi i\frac{n\upsilon}{N}},$$

where $g_k[n] \equiv g[kN+n], n \in [0, N-1]$

2) Combine two segments $b_{k-1}[n]$ and $b_k[n]$ to form a data block B of length 2N:

$$B = \Big\{g_{k-1}[n]e^{-2\pi i\frac{n\upsilon}{N}}, n = 0 \ldots N-1, \quad g_k[n]e^{-2\pi i\frac{n\upsilon}{N}}, n = 0 \ldots N-1\Big\}$$

$$= \Big\{g[(k-1)N+n]e^{-2\pi i\frac{n\upsilon}{N}}, n = 0..2N-1\Big\}$$

3) For a fixed center frequency υ, zero pad the filter coefficients $\{a[\cdot]\}$, $n \in [0, N-1]$ by adding N zeros to form a sequence A of length 2N:

$$A = \{a[0], a[1], \ldots a[N-1], 0,0,0 \ldots 0\}$$

4) Compute 2N-point FFT of A and B

$$\tilde{B} \equiv FFT(B) = G(j + 2\upsilon)$$

$$\tilde{A} \equiv FFT(A) = \sum_{n=0}^{2N-1} a[n] \cdot e^{-2\pi i\frac{nj}{2N}}$$

$$= \sum_{n=0}^{N-1} a[n] \cdot e^{-2\pi i\frac{n(j/2)}{N}}$$

5) Then compute

$$\widetilde{AB}[j] = \sum_{n=0}^{N/\beta-1} \tilde{B}[j+2n\beta] \cdot \tilde{A}[j+2n\beta]$$

Compute $C = IFFT_{2\beta}(\widetilde{AB})$ using $2\beta -$ point IFFT. The second half of the resulting signal C is the DOST for infinite-length signals: $S[l,k] = S[\upsilon,\beta,\tau]$, where υ is a fixed center frequency and l covers all the time points in the k-th sampling time interval in $\{kN + lN/\beta, l \in [0, \beta-1]\}$.

6) Repeat Steps 3-6 to obtain $S[l,m]$ for all center frequency points $\upsilon = \upsilon[m]$ and finish the computation for the k-th signal segment.
7) Repeat Steps 1-7 to obtain the DOST for different segments of an infinite length signal.

Similar to the DST, in order to compute the DOST with the window function centered at zero as shown in Equation (6), we need to recalibrate the results. For the window function : $w'[n,m] = w[n-\tau, m]$, the recalibrated DST is given as $S'[l,m] = S[l-\tau, m]$.

IV. Numerical Performance Evaluations For The DOST Of Infinite-Length Signals

Fig. 1 compares the performance of the infinite-length and finite-length DOST for an infinite-length signal defined as

$$\cos\Big(2\pi\big(\tfrac{24}{256}t + 4\cos\big(2\pi\tfrac{0.6}{256}t + 2.4\pi\big)\big)\Big),$$

whose frequency changes periodically over time. Fig. 1a) shows a 384 samples points of the infinite-length signal for $t \in [0s, 383s]$. The sampling rate is 1 Hz. In Fig. 1b), we compute the DOST for the infinite-length signal segment-by-segment using the proposed Algorithm 1. Each segment is of length 256. The magnitude of the resulting time-frequency spectrum of the signal as displayed in Fig. 1b). The window functions used are similar to the Gaussian functions and have compact support, centered at $\tau = 128$. The window width decreases as the frequency value increases. For each signal segment of length N=256, the frequency sampling interval increases, and the temporal sampling interval decreases as the center frequency value increases. Hence for different frequency bands, the lengths of the FFTs used in the DOST are different: those for higher frequency bands are longer and those for lower frequency bands are shorter. Fig. 1c) shows the result calculated by the conventional finite-length DOST. The signal segmentation, the window function and the other parameters are the same as used in Fig. 1b). The center of the window is zero. As shown in Fig. 1c), obvious border effect can be observed at the intersection of the two segments.

Note that in order to be comparable, the value of the DOST sampled at one time-frequency point is displayed as a sub-matrix whose column and row sizes are determined by corresponding sampling time intervals and frequency sampling intervals, respectively. The intensity values in gray show the magnitudes of the DOST spectra.

The major difference between the finite-length and infinite-length DOST is that the infinite DOST maintains the absolute-reference Fourier phase and hence it removes the border artifacts at the intersections of two segments, while the finite-length DOST does not.

The computational complexity of the DOST for an infinite-length signal is only influenced by the length of the signal segment needed to be processed. For a signal segment of length N, we need less than $8N\log_2 N + 2N + 6$ complex multiplications. Hence, the average number of complex operations for each sampling point is $8\log_2 N + 2$. In our example, the length of the segment is $N = 256$, computing the DOST for each time point needs 42 complex multiplications, compared to 2598 for the DST. And this number stays the same no matter how long the signal to be processed is. Hence it is feasible to realize the fast DOST computation in real-time systems.

V. Discussions And Conclusions

By sampling the time-frequency domain of the continuous Stockwell transform, we derive the new formulation of the DOST for infinite-length signals. We show that the conventional ST for finite-length signals is a special case in the formulation. The infinite-length DOST proposed in this paper not only preserves absolute-reference phase, but also eliminates boundary effects. It allows flexible designs of computational schemes that are feasible for real-time applications.

We also revealed that the conventional definition of the DOST suffers from boundary wrapping effects at the two ends because it implicitly treats a signal of finite-length as a periodically extended signal. This may cause distortion and misinterpretation of the time-frequency spectrum. On the other hand, the infinite-length DOST formulation is defined to process any infinite-length signals, periodic or non-periodic, without boundary effects occurred in the spectrum.

When processing infinitely long or large size signals, it is impractical to process the signal as a whole. Normally segment-by-segment implementation is more practical. Due to boundary effects of the finite-length DOST, however, spectra cannot be accurately obtained at the intersections of adjacent segments. Accurate spectrum can be only computed by processing the whole signal. For a signal of length L, the total computational complexity of the conventional DOST is O(2LlogL). That is, the average computational complexity for each data point is O(2logL). As the signal length increases, the computation requirement becomes possible beyond real-time processing capability of any processor.

In the proposed segment-by-segment implementations of the infinite-length DOST, we utilize the FFT-based FIR filters to compute the spectrum of each segment from two adjacent segments. The resulting overall spectrum is precisely equivalent to the spectrum given by the definitions of the infinite-length DOST. If the length of each segment is N, the average computational complexity for each data point is $O(8\log N)$. These properties are critical for real-time applications.

Even though our algorithm has one data block time delay, this is considered reasonable in many real-time applications, such as telecommunication, radar and GPS systems.

In general, FFT of a power of 2 points is computationally more efficient and most convenient to implement in both software and hardware. Hence the proposed numerical implementations are based on the segment length of a power of 2. However, we can further extend our work to utilize numerous recent developments in fast Fourier transforms [20, 21] to handle arbitrary segment lengths or sparse signals. In the future, we will integrate the theoretical framework of the GDST [13, 22] to generalize the proposed transforms for infinite-length signals. This work will enable us to flexibly adjust the width of window functions and select optimal frequency resolutions adaptive to a specific signal. With that, we aim to further reduce computational complexity and make it more valuable for time-frequency analysis in applications arisen from medicine, remote sensing, and engineering.

References

[1] R. G. Stockwell, L. Mansinha, and R. P. Lowe, "Localization of the complex spectrum: The S transform," IEEE Trans. Signal Processing, vol. 44, no. 4, pp. 998-1001, April.1996.

[2] L. Mansinha, R. G. Stockwell, R. P. Lowe, M. Eramian, and R. A. Schincariol, "Local S-spectrum analysis of 1-D and 2-D", Phys Earth Plan Interiors. 103, pp. 329-336, 1997.

[3] J. Gao, W. Chen, Y. Li, T. Fang, "Generalized S-transform and seismic response analysis of thin interbedss surrounding regions by GPS," Chinese Journal of Geophysics, vol. 46, no. 4, pp. 759-769, 2003.

[4] H. Zhu, B. G. Goodyear, M. L. Lauzon, R. A. Brown, G. S. Mayer, L. Mansinha, A. G. Law, and J. R. Mitchell, "A new local multiscale Fourier analysis for MRI," Med. Phys., vol. 30, no. 6, pp. 1134-1141, 2003

[5] Y. Zhang, H. Zhu, J. R. Mitchell, F. Costello, and L. M. Metz, "T2 MRI texture analysis is a sensitive measure of tissue injury and recovery resulting from acute inflammatory lesions in multiple sclerosis," NeuroImage, vol. 47, no. 1, pp. 107-111, Aug. 2009

[6] G. A. Oldenborger, R. A. Schincariol, and L. Mansinha, "Space local spectral texture segmentation applied to characterizing the heterogeneity of hydraulic conductivity," Water Resources Res., vol. 38, no. 8, pp. 29_1-29_11, Aug. 2002

[7] R. G. Stockwell, W. G. Large, and R. F. Milliff, "Resonant inertial oscillations in moored buoy ocean surface winds," Tellus A, vol. 56, no. 5, pp. 536-547, Oct. 2004.

[8] J. B. Reddy, D. K. Mohanta, and B. M. Karan, "Power system disturbance recognition using wavelet and S-transform techniques," International Journal of Emerging Electric Power Systems, vol. 1, pp. 1007, 2004

[9] R. G. Stockwell, "A basis for efficient representation of the S-transform," Digital Signal Processing, vol. 17, no. 1, pp. 371-393, Jan. 2007.

[10] S. Drabycz, R.G. Stockewll, and J.R. Mitchell, "Image texture characterization using the discrete orthonormal S-transform," Journal of Digital Imaging, vol. 22, no. 6, pp. 696-708, Dec. 2009.

[11] Y. Wang, and J. Orchard, "Fast discrete orthonormal Stockwell transform," SIAM J. Sci. Comput., vol. 31, no. 5, pp. 4000–4012, 2009.

[12] R. A. Brown, "A general description of linear time-frequency transforms and formulation of a fast, invertible transform that samples the continuous S-transform spectrum nonredundantly," IEEE Trans. Signal Processing, vol. 58, no. 1, pp. 281-290, Jan. 2010.

[13] Y. Yan, and H. Zhu, "The generalization of discrete Stockwell transforms," in EUSIPCO, 2011, pp. 1209-1213

[14] C. Liu, "A New Adaptive Multi-Resolution Time-Frequency Representation with Applications in Studying Brain Functions," Ph.D. thesis, Dept. Math. Stat., York Univ., Toronto, ON, 2011.

[15] J. Liu, J. Yao and X. Liu, "Generalized S-transform with adaptive optimized window and its application in seismic signal analysis," Information Technology Journal , vol.12, no. 2, pp. 276-286, 2013.

[16] K. R. Krishnanand and P. K. Dash "A new real-time fast discrete S-transform for cross-differential protection of shunt-compensated power systems," IEEE Transactions On Power Delivery, vol. 28, no. 1, Jan. 2013.

[17] S.R. Samantaray, "Fast S-transform based distance relaying in transmission line," Electric Power Systems Research, vol. 95, pp. 268-274 , Feb. 2013.

[18] E. R. Ferrara, "Fast Implementation of LMS Adaptive Filters," IEEE Trans. Acoustics, Speech, and Signal Processing, vol. ASSP-28, no. 4, pp. 474-475, Aug.1980.

[19] A.V. Oppenheim and R.W. Schafer, Discrete-time signal processing, Prentice-Hall, 1989.

[20] P. Duhamel, "Fast Fourier transforms: A tutorial review and a state of the art", Signal Processingvol. 19, no. 4, pp 259–299, Apr 1990

[21] H. Hassanieh, P. Indyk, D. Katabi and E. Price, "Nearly Optimal Sparse Fourier Transform", arXiv:1201.2501v2 [cs.DS] 6 Apr 2012

[22] Y. Yan, H. Zhu, "The GDST Frame and Inverse Transforms," 2019 IEEE International Conference on Signal, Information and Data Processing (ICSIDP), Chongqing, China, 2019, pp. 1-6, doi: 10.1109/ICSIDP47821.2019.9173153.

[23] Y. Yan, H. Zhu, "The Discrete Stockwell Transforms for Infinite-Length Signals and Their Real-Time Implementations," ICASSP 2020 - 2020 IEEE International Conference on Acoustics, Speech and Signal Processing (ICASSP), Barcelona, Spain, 2020, pp. 5810-5814, doi: 10.1109/ICASSP40776.2020.9054198.